Quantum Interferometry in ρ^0 Production in Ultra-Peripheral Heavy Ion Collisions

Spencer R. Klein[a], for the STAR Collaboration

[a] Lawrence Berkeley National Laboratory, Berkeley, CA 94720

Abstract.

In ρ^0 photoproduction in ultra-peripheral heavy ion collisions, either ion can be the photon emitter or the target. The two possibilities are indistinguishable, and they should be able to interfere, reducing rho^0 production at low transverse momentum, $p_T < \hbar/\langle b \rangle$, where $\langle b \rangle$ is the median impact parameter.

The two ρ^0 production points are separated by $\langle b \rangle \approx 18 - 46$ fm, while the ρ^0 decay before travelling 1 fm. The two decay points are well separated in space-time, so the decays proceed independently and any interference must involve the final state $\pi^+\pi^-$. This requires a non-local wave function.

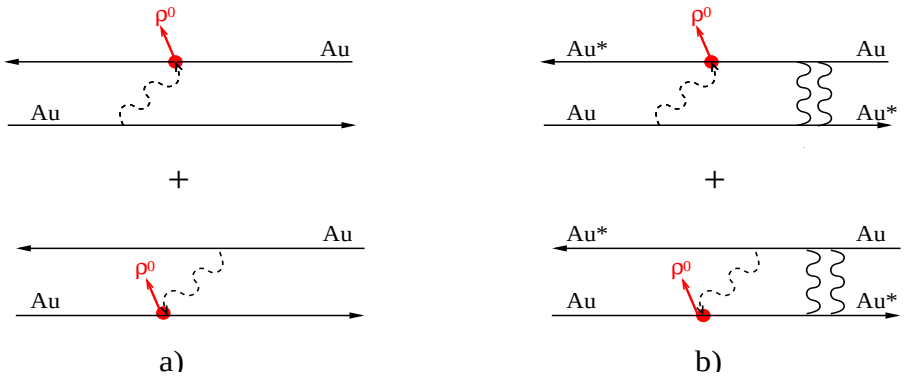

Figure 1. (a) The two possibilities for exclusive ρ^0 production. These two diagrams may be accompanied by mutual Coulomb excitation, as in (b). Different time orderings are not shown in (b), but do not affect the interference.

1. Introduction

ρ^0 may be produced electromagnetically (via photoproduction) in distant interactions between ultra-relativistic heavy ions. In these ultra-peripheral collisions (UPCs) [1], a photon from the electromagnetic field of one nucleus fluctuates to a quark-antiquark pair, which then scatters elastically from the other nucleus, emerging as a vector meson [2]. Elastic scattering is colorless, and can be described in terms of soft Pomeron exchange. For light mesons like the ρ^0, the cross section rises slowly with the photon energy k. For small momentum transfers, the elastic scattering is coherent over the entire nuclear target, greatly increasing the cross section. For heavy mesons, the scattering cross section scales as the atomic number A^2, while for lighter mesons like the ρ^0, a Glauber calculation finds that shadowing reduces the dependence to approximately $A^{5/3}$ [3, 4].

The large photon flux and the coherent scattering lead to a large cross section for ρ^0 production. For 200 GeV per nucleon Au-Au collisions at RHIC, the cross section for ρ^0 production is 590 mb, or about 8% of the hadronic cross section [3]. The STAR collaboration has already measured ρ^0 production in Au-Au collisions at an energy of 130 GeV per nucleon [5]. The cross sections agreed with the Glauber calculations.

The elastic scattering is mediated by the strong force, and so has a short range [6]. The ρ production is localized to within 1 fm of the two ions. Figure 1a shows the two possibilities: either nucleus 1 emits a photon which scatters off nucleus 2, or vice versa. These two possibilities are indistinguishable, and are related by a parity transformation. Vector mesons have negative parity, so the two amplitudes subtract, with a transverse momentum (p_T) dependent phase factor to account for the separation. The cross section is [7]

$$\sigma = \left|A_1 - A_2 \exp\left(ip_T \cdot b\right)\right|^2 \tag{1}$$

where A_1 and A_2 are the amplitudes for ρ^0 production from the two directions. At mid-rapidity $A_1 = A_2$ and

$$\sigma = \sigma_0(b)\left[\left(1 - \cos\left(p_T \cdot b\right)\right]\right. \tag{2}$$

where $\sigma_0(b)$ is the cross section without interference. The system acts as a 2-slit interferometer, with slit separation b [8]. Of course, b is unmeasurable, and the

observed p_T spectrum is obtained by integrating Eq. (1) over all b, subject to the constraint that there are no hadronic interactions (roughly equivalent to $b > 2R_A$). The cross section is suppressed for $p_T < \hbar/\langle b \rangle$, where $\langle b \rangle$ is the median impact parameter. Interestingly, for photo

The ρ decay distance, $\gamma\beta c\tau < 1$ fm is far less than $\langle b \rangle \approx 46$ fm. The ρ^0 decay before the amplitudes from the two sources can overlap, making this an interesting test of quantum mechanics [9].

The coupling constant $Z\alpha$ (where $\alpha \approx 1/137$ is the electromagnetic coupling constant) is large, so multiple interactions between a single ion pair are common. the ρ^0 production may be accompanied by mutual Coulomb excitation, as in Fig. 1b. Each ion emits a photon, which excites the other nucleus, usually to a giant dipole resonance (GDR). The resonance decays by emitting one or more neutrons. These neutrons are a clear experimental signature for nuclear dissociation.

The mutual Coulomb dissociation also 'tags' collisions with moderate impact parameters, $2R_A < b <\approx 30$ fm [10]. As long as $k < \gamma\hbar/b$, the photon flux drops as $1/b^2$. For a single photon reaction like ρ^0 production, the production probability $P(b)$ follows the same scaling. For n-photon interactions, $P(b) \approx 1/b^{2n}$ [11] so the median impact parameter is much smaller and interference is visible at larger p_T.

Except for the shared impact parameter, the photon exchange reactions are independent [11]. The cross section for ρ^0 production with mutual Coulomb dissociation is

$$\sigma = \int d^2b P_\rho(b) P_{2EXC}(b)[1 - P_{had}(b)] \tag{3}$$

where $P_\rho(b)$ and $P_{2EXC}(b)$ are the probabilities for ρ^0 production and mutual excitation respectively. Here, $P_{had}(b)$ is the probability of having a hadronic interaction; the last term has an effect similar to setting a minimum impact parameter $b_{min} = 2R_A$. For gold ions, $P_\rho(2R_A) \approx 1\%$ and $P_{2EXC}(2R_A) \approx 30\%$, so the probability of multiple interactions is substantial. Through the smaller bs, the photon spectra in multi-photon interactions are harder than for single photon reactions.

2. The STAR Detector

The Solenoidal Tracker at RHIC (STAR) studies heavy-ion and polarized proton collisions at the RHIC collider Brookhaven National Laboratory. STAR is optimized for high-multiplicity final states, but it is also effective for 2-4 charged particle final states from UPCs. STAR collected UPC data in gold-gold collisions at energies of 130 GeV per nucleon (in 2000) and 200 GeV per nucleon (in 2001). STAR has also studied ρ^0 photoproduction in 200 GeV per nucleon deuteron on gold collisions [12]. The ρ^0 interference analysis uses the 2001 gold-gold collisions dataset.

Charged particles are reconstructed in a 4.2 meter long, 4 meter diameter time projection chamber (TPC) [13]. This data was taken with the TPC in a 0.5 T solenoidal magnetic field. The $\pi^\pm$ reconstruction efficiency is high for tracks with transverse momentum $p_T > 100$ MeV/c and pseudorapidity $|\eta| < 1.15$. The track position and specific energy loss, dE/dx were measured at 45 points for high momentum charged particles with $|\eta| < 1$. The TPC is surrounded by 240 scintillator slats covering $|\eta| < 1$, comprising the central trigger barrel (CTB). Two zero degree calorimeters (ZDCs) are located 18 m upstream and downstream of the interaction point. These calorimeters are sensitive to neutrons from mutual Coulomb dissociation [14].

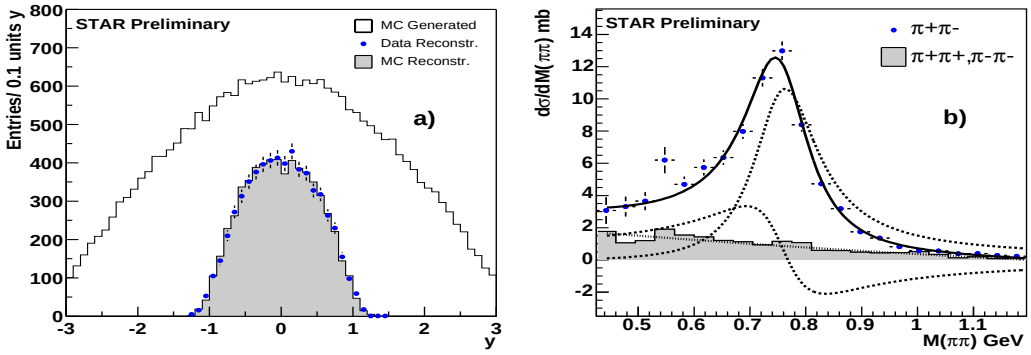

Figure 2. The (a) rapidity and (b) $\pi\pi$ invariant mass spectra of ρ^0 using data from the minimum bias trigger. The mass is fit to to a Breit-Wigner function for the ρ^0, plus a Söding term due to interference with a direct $\pi\pi$ component. The combinatoric hadronic background is also shown.

Two different triggers [15] were used to study interference. The 'topology' trigger selected events with 2 roughly back-to-back tracks in the CTB. It divided the CTB into 4 quadrants: north, south, top and bottom, and required hits in the north and south quadrants. The top and bottom regions were used as vetoes to reject cosmic rays.

The minimum bias trigger selected events with one or more neutrons in each ZDC. The ZDC signals were required to occur within 1 nsec, restricting these events to the central 30 cm of the TPC. Data from both triggers was processed identically, except that events from the CTB based trigger were distributed more broadly along the TPC axis, and consequently, were accepted in a broader range.

3. ρ^0 Production

UPC ρ^0 production has a distinctive signature - two oppositely charged tracks with small net p_T. We select events with exactly 2 primary tracks that form a vertex. The vertexing procedure considers all of the tracks in an event, and rejects tracks that are inconsistent with coming from a single vertex. We allow a few non-primary background tracks in the TPC. The topology and minimum bias data were treated identically, except that allowance was made for the different distribution of the accepted event production points. This study used about 1.5 million minimum bias and about 1.7 million topology triggers. This analysis will study the p_T spectra of produced ρ^0.

Figure 2a shows the rapidity distribution of the coherent ρ^0 (pairs with $p_T < 150$ MeV/c). The points (data) are in excellent agreement with a calculation based on the soft Pomeron model and our detector simulation.

Figure 2b shows the $\pi\pi$ invariant mass, $M_{\pi\pi}$ for the sample. The data is fit to a relativistic Breit-Wigner for the ρ^0, plus a Söding term to account for the interference with direct $\pi^+\pi^-$ production [16]. The interference shifts the peak of the distribution to lower $M_{\pi\pi}$. The direct $\pi\pi$ to ρ ratio agrees with the STAR 130 GeV analysis [5] and with studies by the ZEUS collaboration in γp interactions [17]. However, with the nuclear coherence, the STAR data is at smaller $|t|$ than the ZEUS analysis, so the two results may not be directly comparable [18].

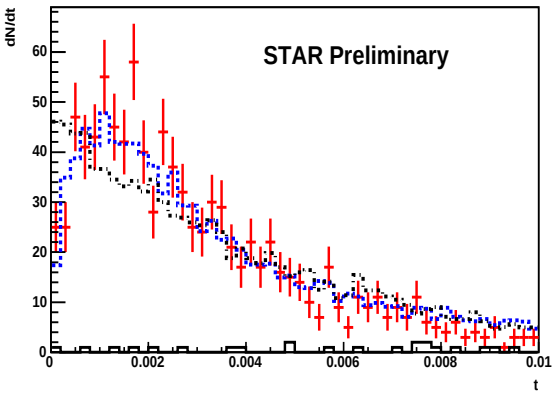

Figure 3. Raw (uncorrected) $t_\perp$ spectrum for ρ^0 sample for $0.1 < |y| < 0.5$ for the topology data. The points (red) are the data. The dashed histogram (blue) is a simulation that assumes that there is interference, while the dot-dash histogram (black) is based on a calculation without interference. The solid black histogram with very few counts is the like-sign background.

4. ρ^0 Interferometry

Stringent event selection criteria were used to select a clean, low-background sample for the ρ^0 interference study. Events were required to have exactly two tracks with a vertex within 50 (100) cm longitudinally of the center of the TPC for the minimum bias (topology trigger) sample. ρ^0 candidates with $|y| < 0.1$ were eliminated to avoid possible contamination from cosmic rays. The pairs were required to have 550 MeV $< M_{\pi\pi} <$ 920 MeV. The minimum mass cut removed most of the hadronic backgrounds, which are concentrated at low $M_{\pi\pi}$. These cuts reduced the like-sign pair background to a few percent. With these cuts, the background from misidentified two-photon reactions like $\gamma\gamma \to e^+e^-$ should be very small. The sample still includes direct pions, which should have the same spin/parity and quantum mechanical behavior as the pion pairs from ρ decay. We do not distinguish between the two sources.

The magnitude of the interference depends on the ratio of the amplitudes for ρ production on the two nuclei. Away from $y = 0$, the photon energies for the two photon directions differ, $k_{1,2} = M_V/2 \exp(\pm y/2)$; the amplitudes differ and the interference is sub-maximal. Although it is not expected in the soft-Pomeron model, the the photon energy difference could introduce a small ρ^0 production phase difference, which could affect the interference [2]. This analysis focuses on the region near mid-rapidity where any phase difference should be small. A Monte Carlo is used to find the interference for different rapidity ranges [3, 7].

We study the p_T spectra using the variable $t_\perp = p_T^2$. At RHIC energies, the longitudinal component of the 4-momentum transfer is small, so $t \approx t_\perp$. Without interference, the spectrum $dN/dt \propto \exp(-bt)$ [7, 19].

Figure 3 compares the uncorrected minimum bias data for $0.1 < |\eta| < 0.5$ with two simulations, with and without interference. Both simulations include the detector response. The data has a significant downturn for $t < 0.001$ GeV^2, consistent with the $\langle b \rangle = 18$ fm expected for a ρ^0 accompanied by mutual excitation [11]. This data matches calculation with interference, but not the no-interference result.

The efficiency corrected data are shown in Fig. 4. Minimum bias and topology

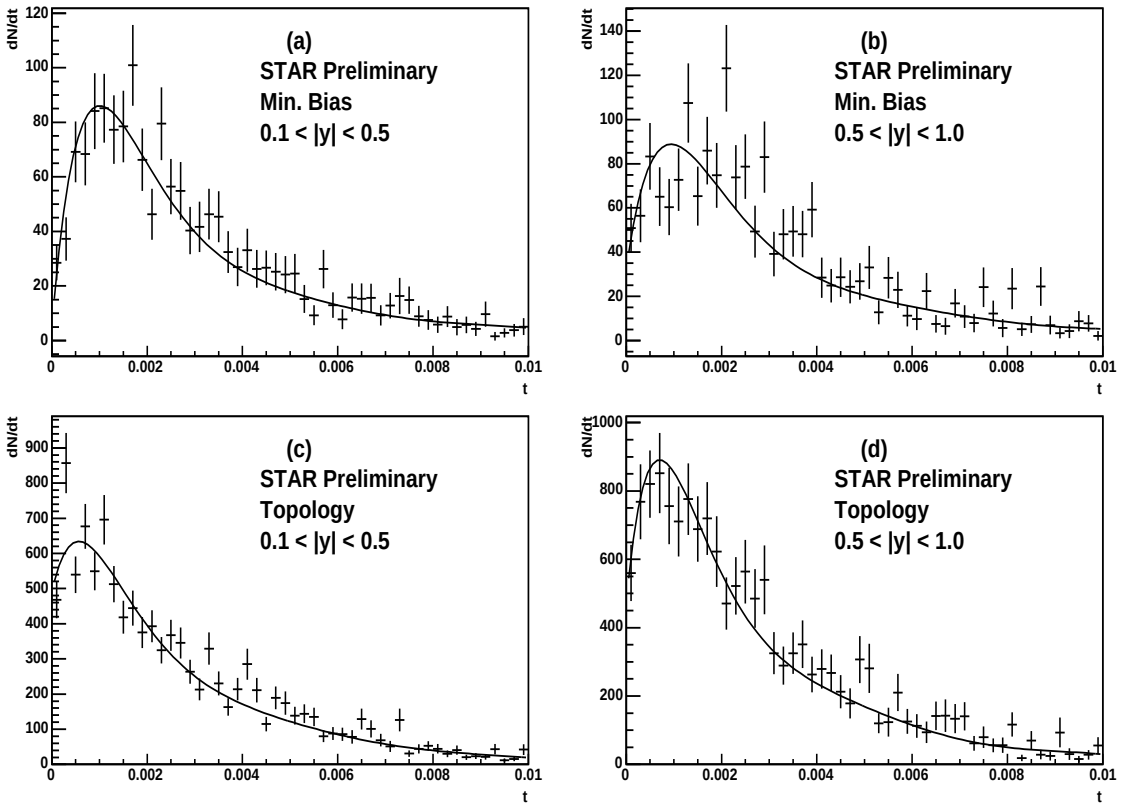

Figure 4. Efficiency corrected $t_\perp$ spectrum for ρ^0 from (a) mutual dissociation with $0.1 < |y| < 0.5$, (b) mutual dissociation with $0.5 < |y| < 1.0$, (c) topology trigger with $0.1 < |y| < 0.5$ and (d) topology trigger with $0.5 < |y| < 1.0$. The points are the data, while the solid line is the result of the fit to Eq. 4.

data are shown separately, each with two rapidity bins: $0.1 < |y| < 0.5$ and $0.5 < |y| < 1.0$. The efficiency is independent of p_T. However p_T smearing (resolution) does affect the spectrum slightly; the efficiency correction removes this. The ρ^0 p_T resolution is about 9 MeV/c, while the 1st t bin covers 0 to (15 MeV/c)^2. Interference depletes the first few bins, but feed down from the higher t bins partially repopulates them.

The data is fit to the 3-parameter form:

$$\frac{dN}{dt} = a\exp(-bt)[1 + c(R(t) - 1] \tag{4}$$

where $R(t) = Int(t)/Noint(t)$ is the ratio of the Monte Carlo t-spectra with and without interference. Here, a is the overall normalization, the slope $b \approx R_A^2$, and c is the degree of spectral modification; $c = 0$ corresponds to no interference while $c = 1$ is the calculated interference. This functional form separates the interference (c) from the nuclear form factor (b).

Table 1 gives the results of the fits. At small-rapidities the amplitudes from the two directions are similar and the interference reduces the cross section at $p_T = 0$ by more than at larger rapidities. In the minimum bias data, the interference extends to

Trigger	|Rapidity|	b (GeV^{-2})	c	χ^2/DOF
Minimum Bias	$0.1-0.5$	301 ± 14	1.01 ± 0.08	50/47
Minimum Bias	$0.5-1.0$	304 ± 15	0.78 ± 0.13	73/47
Topology	$0.1-0.5$	361 ± 10	0.71 ± 0.16	81/47
Topology	$0.5-1.0$	368 ± 12	1.22 ± 0.21	50/47

Table 1. Results of the fits to the two datasets for the two rapidity bins.

higher p_T than the topology data because the former has a smaller $\langle b \rangle$.

The 4 c values are consistent within errors; the weighted average is $c = 0.93 \pm 0.06$. The b values for the minimum bias and exclusive ρ^0 data differ by 20%: 364 ± 7 GeV^{-2} for the exclusive ρ versus 303 ± 10 GeV^{-2} for the Coulomb breakup events.

The different b values may be attributed to the different impact parameter distributions caused by the nuclear breakup tagging in the minimum bias data. The photon flux depends on the impact parameter as $1/b^2$. When $b \approx \mathrm{few} R_A$, ρ are more likely to be produced on the side of the target near the photon emitter than on the far side. ρ^0 production is concentrated on the near side, leading to a smaller effective production volume and the smaller b. This near-side skewing affects the interference slightly, but is not included in current calculations.

Systematic errors come from a variety of sources. We have studied the effect of detector distortions (primarily p_T smearing) by turning off the detector simulation and comparing raw simulations with reconstructed data. This lowered c by 18%; if the detector simulation is 75% correct (a very conservative assumption), then detector effects are a less than 5% systematic uncertainty. Minor systematic uncertainties come from backgrounds and the fitting procedure. We have compared the data and simulations for a variety of kinematic and detector-based variables, and found good agreement. We estimate a preliminary experimental systematic uncertainty of 8%.

This analysis depends on the shape of $R(t)$, which is calculated following Ref. [7]. There are some simplifications in Ref. [7]. The calculation averages the photon flux over the surface of the nucleus, rather than incorporating the proper $1/b^2$ weighting. This may partly explain the relatively poor fit for the large-$|y|$ Coulomb breakup fit. We estimate that the effective impact parameter should be within 10% of the actual ion-ion separation for the coulomb breakup data, and 3% for the exclusive ρ. The uncertainties in the calculations should be at most a 15% effect. With this, the interference is $93 \pm 6(stat.) \pm 8(syst.) \pm 15(theory)$% (STAR preliminary) of that expected.

The ρ decays rapidly, with $\gamma\beta c\tau \ll \langle b \rangle$ and the two ρ decay points are well separated in space-time. In the usual space-time picture, the decays occur independently, and any interference must involve the final state $\pi^+\pi^-$. Interference must involve identical final states from the two sources. However, given the large available phase space for the decays, this is very unlikely for independent decays.

One interpretation of this result is given in Ref. [9]. In it, the interference occurs because the post-decay wave function includes amplitudes for all possible final states, then the amplitudes for identical states subtract, and the interference is visible. Because of the two sources, the $\pi^+\pi^-$ wave function is non-factorizable, and thus exhibits the Einstein-Podolsky-Rosen paradox [20]. We find that the decoherence, $1-c$, due to environmental or other factors is less than 43% at the 90% confidence level.

5. Conclusions

The STAR collaboration has studied exclusive ρ^0 photoproduction and ρ^0 photoproduction accompanied by nuclear excitation. The cross sections and rapidity distributions match the predictions of the soft Pomeron model.

Production at low$-p_T$ is suppressed, as expected if ρ^0 production at the two ions interferes destructively. The suppression is $93 \pm 6(stat.) \pm 8(syst.) \pm 15(theory)\%$ of that expected. The decoherence is less than 43% at a 90% confidence level.

We thank Tony Baltz and Joakim Nystrand for help with the theoretical calculations. This work was supported by the U.S. DOE under contract number DE-AC-03-76SF00098.

6. References

[1] G. Baur *et al.*, Phys. Rep. **364**, 359 (2002); F. Krauss, M. Greiner and G. Soff, Prog. Part. Nucl. Phys. **39**, 503 (1997).
[2] T. H. Baur *et al.*, Rev. Mod. Phys. **50**, 261 (1978).
[3] S. Klein and J. Nystrand, Phys. Rev. **C60**, 014903 (1999).
[4] L. Frankfurt, M. Strikman and M. Zhalov, Phys. Rev. **C67**, 034901 (2003).
[5] C. Adler *et al.*, Phys. Rev. Lett. **89**, 272302 (2002).
[6] B. Müller and A. J. Schramm, Nuclear Physics **A523**, 677 (1991).
[7] S. Klein and J. Nystrand, Phys. Rev. Lett. **84**, 2330 (2000).
[8] An analagous two-slit interferometer is described by T. Sudbery in *Quantum Concepts in Space and Time*, ed. R. Penrose and C. J. Isham, (Oxford, 1986).
[9] S. Klein and J. Nystrand, Phys. Lett. **A308**, 323 (2003).
[10] A. Baltz, S. Klein and J. Nystrand, Phys. Rev. Lett. **89**, 012301 (2002).
[11] G. Baur *et al.*, Nucl. Phys. **A729**, 787 (2003).
[12] F. Meissner and V. B. Morozov, nucl-ex/0307006 (2003).
[13] M. Anderson *et al.*, Nucl. Instrum. & Meth. **A499**, 659 (2003); M. Anderson *et al.*, Nucl. Instrum. & Meth. **A499**, 679 (2003).
[14] C. Adler *et al.*, Nucl. Instrum. & Meth. **A470**, 488 (2001).
[15] F. S. Bieser *et al.*, Nucl. Instrum. & Meth. **A499**, 766 (2003).
[16] P. Söding, Phys. Lett. **19**, 702 (1966).
[17] J. Breitweg *et al.*, Eur. Phys. J. **C15**, 1 (2000).
[18] Mark Strikman, private communication (2003).
[19] M. Alvensleben *et al.*, Phys. Rev. Lett. **24**, 792 (1970).
[20] A. Einstein, B. Podolsky and N. Rosen, Phys. Rev. **47**, 777 (1935).